Calibration and Evaluation of Body Interaction Effects for the Enhancement of a Body-Borne Radio Direction Finding System

Arian Lalezari[1,2], Farzin Lalezari[2] and Dejan S. Filipović[1]

[1] Department of Electrical and Computer Engineering,
University of Colorado, Boulder, CO 80309-0425, USA
lalezari@colorado.edu, dejan@colorado.edu

[2] FIRST RF Corporation, Boulder, CO 80301-2307, USA
alalezari@firstrf.com

Abstract: A method of moments (MoM) based computational study and design of a body-borne direction finding (DF) system is investigated in this paper. A baseline two-sensor DF system is established, and the performance of this system is characterized with measurements and simulation. A cylindrical human body model is then introduced to the system as a passive scatterer. Computer models of the body-borne system are validated using measurements with a prototype human body phantom. A parametric system response study is performed on the most important model variables to identify system stability. A discussion is presented on how these data may be applied to a direction finding function to generate a direction finding solution. This work clearly demonstrates the ability of modern computational electromagnetics tools to accurately and efficiently predict the response of complex physical systems.

Keywords: Direction Finding, Geolocation, Body Interaction, Computational Electromagnetics, FEKO Calibration.

I. INTRODUCTION

Technologies utilizing wireless links are simultaneously growing smaller, more prolific, and operating across larger portions of the radio frequency (RF) spectrum. To identify and locate these devices, there is a corresponding demand from commercial, consumer, and military users for direction finding (DF) and geolocation capabilities that match these trends in size, capability, and bandwidth. To address a further demand for mobility, there is specific interest in extending these capabilities to individual users in body-borne or body-worn systems.

Direction finding techniques have been used in the radio band for almost as long as communications. Several phase-based, amplitude-based, and complex (phase and amplitude) DF techniques exist, and are well-summarized in [1]. Although maritime direction finding techniques were well established as early as 1925 [2], the application of these technologies increased considerably during World War II [3]. Several radio navigation systems including the VHF omni-directional radio range (VOR), Tactical Air Navigation (Tacan), Instrument Landing System (ILS), and Microwave Landing System (MLS) are direct results of these technologies [4]. In these systems, the signals of interest are beacons with characteristics that are known *a priori*, and are used to identify and locate the signal [5].

In this paper, a two-element antenna system is evaluated for application to broadband (100-750 MHz) body-borne radio direction finding and geolocation of unknown signals. In the past, multiple sensors or unique signal characteristics have been required to obtain unambiguous direction finding solutions. In this paper, a baseline two-sensor system is established, and its performance is simulated with EMSS FEKO [6], and validated with measurements. To understand body-borne performance, a passive scatter, the human body, is introduced to the system. Using a cylindrical human body model, the effects of this scatterer on the sensors of the DF system are characterized and validated with measurements of a prototype body phantom. The impact of the human body on the phase and amplitude of the direction finding system response is characterized as a function of frequency and angle of arrival.

After a thorough characterization of the baseline human body model, a multi-variable system response study is used to evaluate the changes of the phase and amplitude of the detected signal in the body-borne environment. In total, twelve system parameters, arranged into four categories (radiator, body, system, and excitation parameters) are studied. Using these data, practical frequency-independent phase and amplitude perturbation thresholds are established for differentiating between system variability and viable signal detections. Using these thresholds, an auto-correlating direction finding function (DFF) [7] to demonstrate how the phase and amplitude measurements of the system can be used to produce direction finding solutions.

By computationally evaluating the performance of a body-borne direction finding system in this paper, several contributions have been made:

- Full-wave simulation of a body-borne radio direction finding system, including sensor performance.
- Broadband characterization of platform interaction effects on a multi-sensor direction finding system using computational modeling.
- Validation of computer models with measurements from physical prototypes.
- Completion of a computational multi-variable parametric system response study to characterize system performance.
- Demonstration of a technique to use the results of the parametric study to establish amplitude and phase thresholds to differentiate between normal system perturbation and signal detections.
- Adaptation and application of an auto-correlating direction finding function to exploit platform interaction effects to generate direction finding solutions.

The remainder of this paper is arranged as follows. In Section II, the baseline two-sensor direction finding system is established, and free-space and body-borne simulations are validated with measurements. The results of a parametric system response study are provided in Section III. Using these data, frequency-independent thresholds are established to differentiate between normal system dynamics and detectable differences in incoming signals. In Section IV, a direction finding function (DFF) is adapted from the literature to demonstrate how these data can be applied to generate phase and amplitude based direction finding systems. Conclusions and future work are summarized in Section V.

II. Modeling

To model a body-borne direction finding system, a two-antenna sensor array is mounted on a cylindrical human body model, as shown in Figure 1(a). In order to satisfy a backpack-mounted integration, the height of the antennas, represented as h, is selected to be 20". Likewise, the spacing between the elements along the y-axis is represented as d, and is selected to be 20".

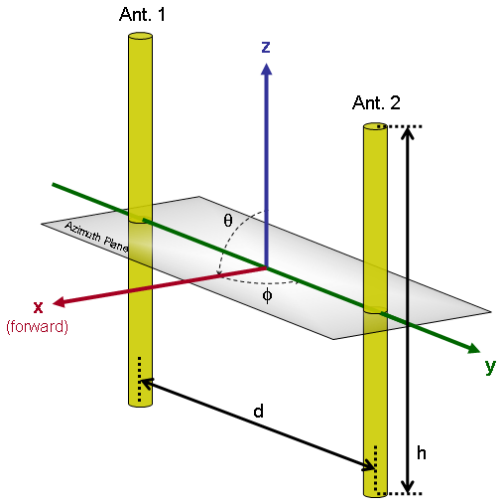

(a) Sensor geometry.

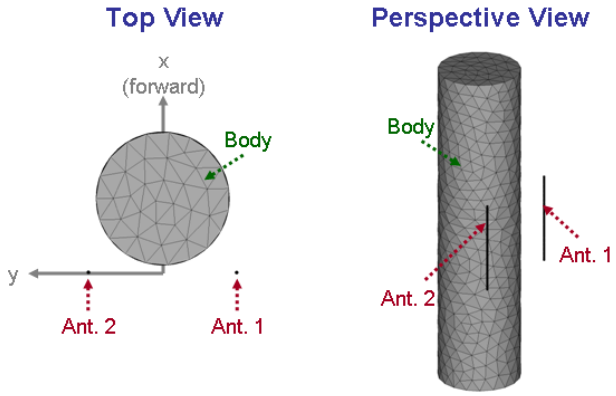

(b) Body-borne system geometry.

Figure 1. Direction finding system geometry.

A. Human Body Model

As seen in Figure 1(b), a commonly used cylindrical human body phantom [8], [9], [10] is adopted in this paper. A dielectric model for this phantom is consistent with the available data at about 300 MHz [11]. This is approximately the geometric mean frequency of the band of interest ($\sqrt{100 \times 750} = 273.9 \approx 300$). A dielectric constant of $\varepsilon_r = 60$ and an electrical conductivity of $\sigma = 0.9$ S/m are chosen. The cylinder has an 18" diameter and is 6' tall. To represent a realistic body integration scheme, the axis of the cylinder is offset by 10" in the positive x-axis (forward) from the center of the antennas. The body model is aligned with the center of the antennas in the y-axis. The antennas and body model are oriented along the z-axis.

B. Modeling

The body-borne direction finding system is simulated using a method of moments code, EMSS FEKO [6]. To emulate operation of a direction finding system, the model is excited by incident plane waves. Signal frequencies from 100-750 MHz in steps of 50 MHz, and angles of arrival from $\phi = -180°$-$180°$ in steps of $5°$, are used. All signals are incident from the azimuthal plane ($\theta = 90°$). The two wire dipole antennas in the DF system are terminated with 50Ω loads. The phase and amplitude of the induced currents across these terminations are used to characterize the system response as a function of frequency and angle of arrival.

C. Validation

For initial modeling validation, the response of the direction finding system is tested in an anechoic chamber. Two center-fed 20" brass dipoles with a diameter of 0.2" are used with 50Ω printed baluns as the sensors. As in simulations, the antenna response is measured when excited by an incident wave. In these measurements, a broadband log-periodic (LP) source antenna is used. Due to anechoic chamber size limitations, only the 300-750 MHz band is measured.

To characterize the individual sensors, measurements of the free-space performance of a single antenna are taken across the band of interest. In FEKO, a wire antenna model is generated with the same height, and simulated across the same band of interest. The data from the measured and computer simulation tests in free space are shown in Figure 2(a) and 2(b) at three frequencies spanning the band of interest. As seen, good correlation between measurement and simulation is obtained. The observed disagreements are due to the effects of the baluns that are required in the measurements, but are excluded from simulation models.

The performance of the sensors in a two-element array configuration is also measured. As in the direction finding system, the reference point for these tests is the mid-point between the antennas. Accordingly, this reference is located along the axis of rotation in measurements, and at the origin in simulation. In this configuration, the antennas are located at $\pm 90°$ in azimuth, as illustrated in Figure 1. Again, the antennas are characterized in free space, such that the only obstruction is the other antenna, which is terminated in a broadband resistive (50Ω) load. Received amplitude and phase data are gathered for both antennas, and measurements of the antenna located at $90°$ azimuth are presented in Figure 3(a) and 3(b). The antenna separation is $d/2 = 10$" from the center of rotation, its received phase varies like $(d/2 \sin\phi)$, where ϕ is the azimuth angle. At the high end of the band, the magnitude of this variation is

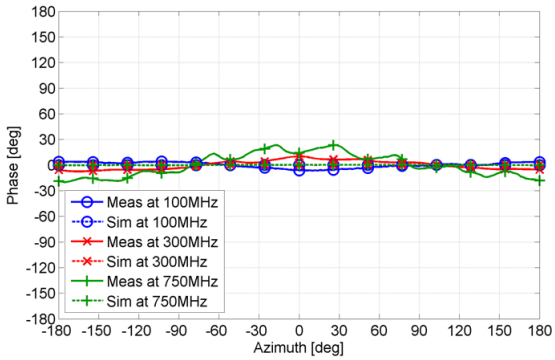

(a) Free space phase.

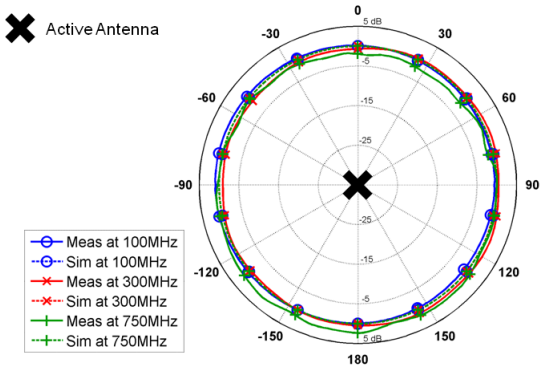

(b) Free space amplitude.

Figure 2. Free space single sensor validation.

approximately $240°$, so the phase has been "unwrapped", so that it may extend beyond $\pm 180°$.

As in the single sensor simulations, there is excellent agreement between simulations and measurements. The spatial dependence exhibited by the system response in Figure 3 is of particular importance. It is this characteristic that will be exploited to generate a direction finding solution.

To evaluate MoM modeling with complex structures, a prototype cylindrical human body phantom is built and tested. Due to limited availability of parts, this model is built with a 12" diameter polyvinyl chloride (PVC) pipe, and is 5' tall. To emulate the dielectric properties (dielectric constant and conductivity) of the human body, a 1% salt water solution is used to fill the model [11]. Two center-fed 20" brass dipoles with a diameter of 0.2" are used with 50Ω printed baluns. The model is tested at an outdoor test facility using a monocone antenna as a source, as shown in Figure 4(a).

As seen in Figure 4(b), a computer model using a cylinder of the same size and shape as the test structure is used for validation. Because of its relatively low dielectric constant, the 0.4" PVC wall thickness is ignored in simulations. To compare the results of the measured and simulated experiments, the relative phase and amplitude

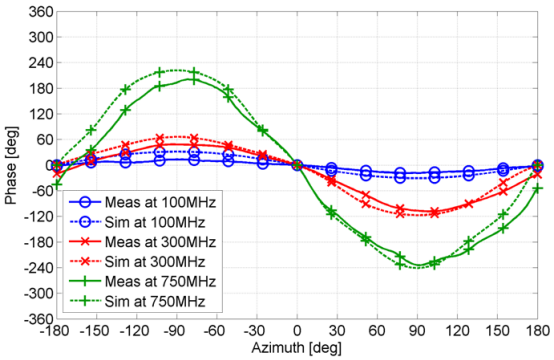

(a) Free space phase.

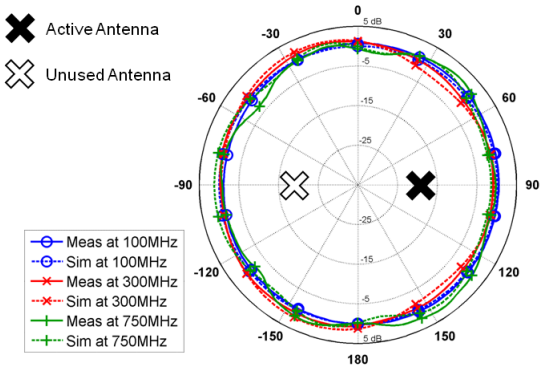

(b) Free space amplitude.

Figure 3. Free space sensor pair validation.

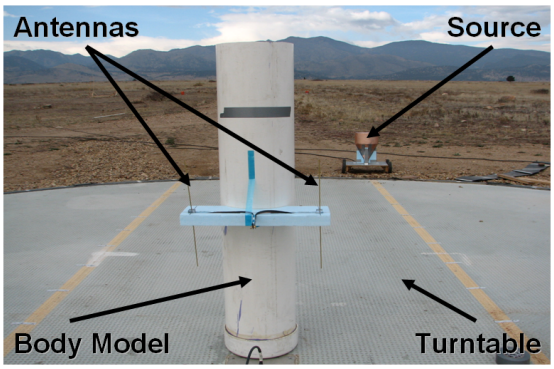

(a) Physical prototype test.

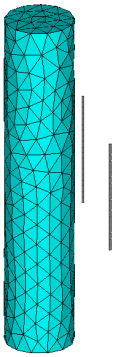

(b) Computer validation model.

Figure 4. Modeling validation configurations.

of signals detected by the two sensors in the system are recorded. Due to restrictions on test frequencies at the outdoor test facility, only the 200-600 MHz band is used. Accordingly, the phases and amplitudes of the system response, as a function of azimuth angle for three different frequencies, are shown in Figure 5.

As seen, there is excellent agreement between measurement and simulation in the available part of the band for both the phase and amplitude of the response.

III. Parametric System Response

While many of the parameters used in the baseline human body and antenna sensor models are favorable for modeling, they are a coarse representation of the real-world realization of the system. Accordingly, the remainder of this study explores the variations in system response to various geometric and model parameters. The objective is to understand how the behavior of the system might be impacted by real-world perturbations of system parameters, so the values by which they are perturbed are chosen to reflect conditions that might be encountered in different realized configurations and/or calibration setups of the system. To determine the variations of the data used by the direction finding system, twelve model parameters are selected. They are divided into four categories, summarized in I.

The alternate values for each of these variables are selected to represent changes to the system that might occur due to normal movement of the user. Accordingly, this study is intended to characterize how the phase and amplitude response of the direction finding system are impacted by normal use of the system. Based on these results, "detection thresholds" are selected. These thresholds allow the direction finding system to differentiate changes in phase and amplitude perturbations that are expected with normal system use from phase and amplitude changes associated with signals from different angles of incidence. That is, any phase and amplitude variation below these thresholds will be attributed to normal use and will establish the system uncertainty, while phase and amplitude differences above these thresholds will be used to differentiate larger changes in the system response, associated with the angle of incidence of an incoming signal. In all cases, at least three values of the variable are selected, mainly one above and one below the nominal configuration value. However, in some cases — when the model geometry precludes two-sided alternate configurations — two values that are both above or below the nominal variable are chosen.

Table I
TWELVE VARIABLE CONFIGURATIONS ARE STUDIED IN A PARAMETRIC STUDY.

Category	Variable	Nominal	Alternate		
Radiator Parameters	Radiator Height	20”	15”	25”	
	Termination Impedance	50Ω	25Ω	75Ω	100Ω
Body Parameters	Body Diameter	18”	15”	12”	
	Body Height	6’	5.5’	6.5’	
	Body ε_r	60	20	40	80
System Parameters	Baseline Separation	20”	18”	22”	
	Baseline Rotation	0°	5°	10°	
	Antenna Z Position	0”	12”	24”	
	Body X Position	10”	8”	12”	
	Body Y Position	0”	1”	2”	
Excitation Parameters	Signal Elevation	90°	105°	120°	
	Signal Polarization	0°	45°	90°	

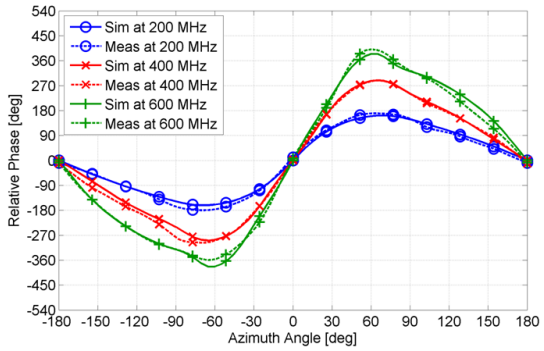

(a) Relative phase of system response.

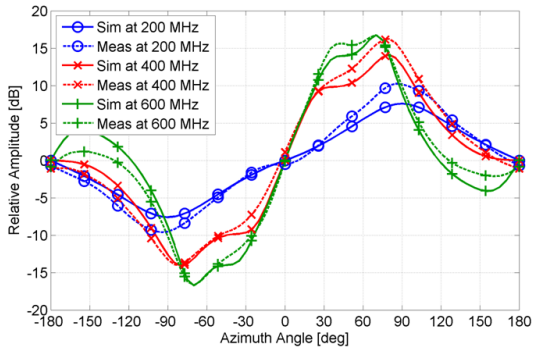

(b) Relative amplitude of system response.

Figure 5. Relative phase and amplitude data from modeling validation.

Frequency-dependent data from the conducted studies are provided for the raw phase and amplitude responses of the direction finding system. As previously shown, the system response at each frequency is a function of incident angle. To represent the distribution of the perturbation to this response across all angles of incidence effectively, these data must be consolidated. If the angular perturbations are considered to lie in some distribution, it is convenient to describe the shape and location of this distribution. Common statistical metrics are used to describe the nominal perturbation (mean), the distribution of the perturbations (standard deviation), and their extent (maximum value) [12].

A. Radiator Parameters

1) Radiator Height: As described in the previous section, the nominal radiator height is 20”. To study the effects of this parameter on the amplitude and phase response of the system, antenna heights of 15” and 25” are compared to the nominal configuration. The frequency-dependent phase and amplitude response perturbations due to the varied radiator height are provided in Figure 6(a) and Figure 6(b), respectively.

Although it is unlikely that the size of the sensors used in any real-world implementation of this system would change length, it is not inconceivable (e.g. due to damage or improper repair or replacement). As previously discussed, the phase and amplitude of the received signal is dependent on the size and shape of these sensors. Accordingly, it is not surprising that there are significant changes in the response of the system when the sensor height is changed. At 15” and 25”, the radiator is resonant at approximately 393 and 236 MHz, respectively. Not surprisingly, there is a correspondingly large perturbation in the system response around these frequencies. The largest perturbation, however, occurs at the high end of the frequency band, driven both by the electrical first anti-resonance of the smaller antenna and the second resonance of the larger antenna. As confirmed by these results, maintaining the expected system performance will be somewhat reliant on maintaining the size and integrity of the sensors.

2) Radiator Termination Impedance: The nominal radiator termination is 50Ω. To study the effects of this parameter on the amplitude and phase response of the system, radiator terminations of 25Ω, 75Ω and 100Ω are compared to the nominal configuration. The frequency-dependent phase and amplitude response perturbations

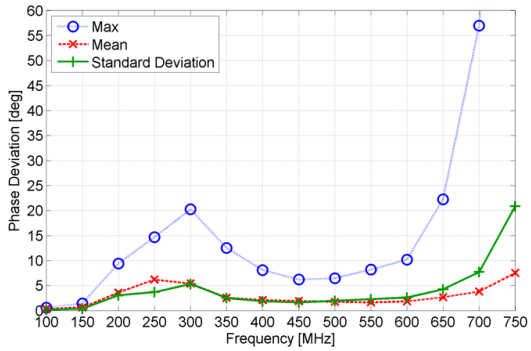

(a) Phase response perturbation.

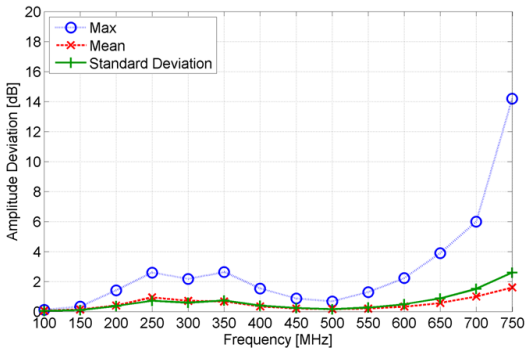

(b) Amplitude response perturbation.

Figure 6. System response to variations of the radiator height.

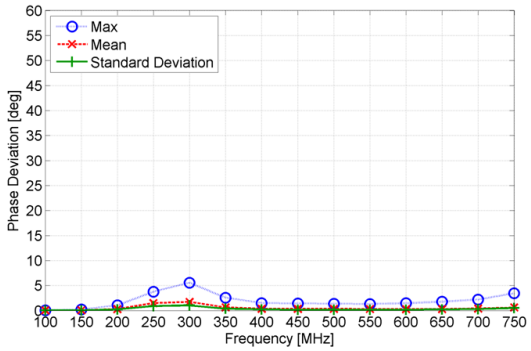

(a) Phase response perturbation.

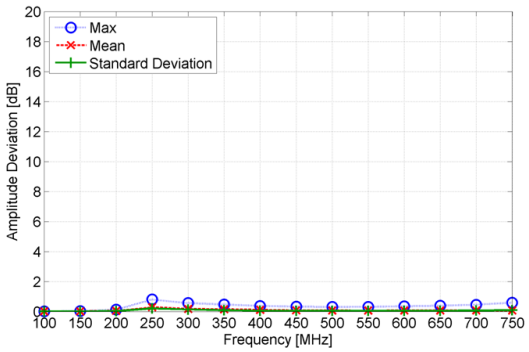

(b) Amplitude response perturbation.

Figure 7. System response to variations of the radiator termination.

due to the varied radiator termination are given in Figure 7(a) and Figure 7(b), respectively.

As previously discussed, the two-sensor system must necessarily use the relative amplitude and phase of the system response to generate a direction finding solution. The system response is collected from the currents excited across the terminated port of the antenna. These currents are proportional to the impedance, so it is not surprising that equally changing the termination impedance of both sensors produces almost no change in the system response, except near resonance, around 300 MHz. Near this frequency, the maximum phase deviation is approximately $5.5°$, and the maximum amplitude deviation is approximately 0.8dB, indicating that the system is relatively insensitive to perturbations of this parameter.

B. Body Parameters

1) Body Diameter: The nominal body diameter is 18". To study the effects of this parameter on the amplitude and phase response of the system, body diameters of 15" and 12" are compared to the nominal configuration. The nominal spacing of the antennas is 20", so body diameters larger than 18" are not studied, as these would engulf the sensors. The frequency-dependent phase and amplitude response perturbations due to the varied body diameter are provided in Figure 8(a) and Figure 8(b), respectively.

As seen, there is a frequency dependence on both the phase and amplitude perturbations. At 750 MHz, the maximum phase perturbation is approximately $115°$, and the maximum amplitude perturbation is approximately 13dB. The standard deviations for these perturbations are approximately $14.5°$ and 2.5dB, respectively, indicating that the maximum perturbations are relatively rare, 5.7σ away from the mean for the phase and over 3.3σ away from the mean for the amplitude. Still, these results indicate that maintaining the expected system performance is reliant on characterizing the body diameter well, and that system calibration needs to be performed for each user.

2) Body Height: The nominal body height is 6'. To study the effects of this parameter on the amplitude and phase response of the system, body heights of 5.5' and 6.5' are compared to the nominal configuration. The body model was selected to represent a tall user, so body heights greater than 6.5' are not studied. The frequency-dependent phase and amplitude response perturbations due to the varied body height are provided in Figure 9(a) and Figure 9(b), respectively.

The frequency dependence of the perturbations due

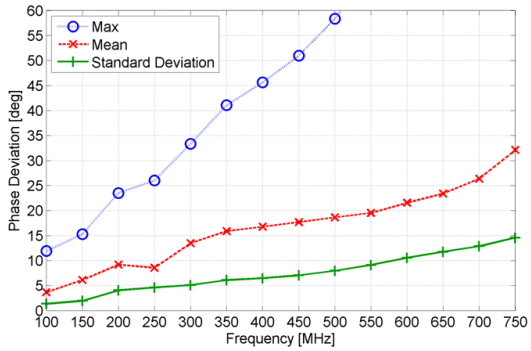

(a) Phase response perturbation.

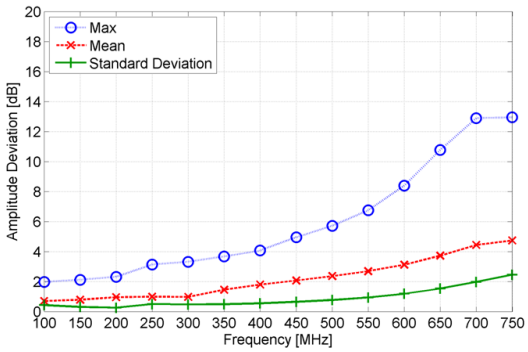

(b) Amplitude response perturbation.

Figure 8. System response to variations of the body diameter.

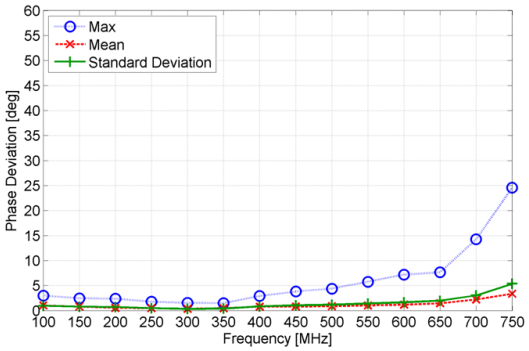

(a) Phase response perturbation.

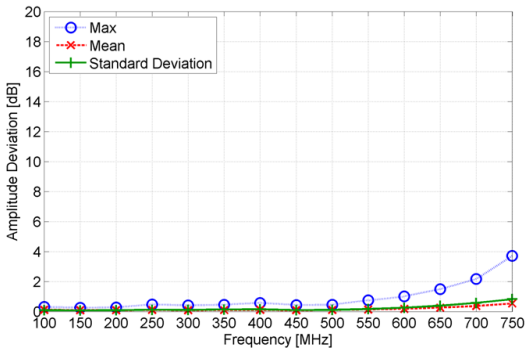

(b) Amplitude response perturbation.

Figure 9. System response to variations of the body height.

to the body height are less pronounced than those associated with the body diameter. Still, the largest maximum perturbations occur at 750 MHz: approximately 24.5° for the phase, and 3.9dB for the amplitude. At over 4σ away from the mean, both maximum perturbation values are rare. This is also reflected in the low mean and standard deviation perturbation values for both the phase and amplitude across the frequency band.

Although the cylindrical human body model provides only a coarse representation of a real user, the height study summarized here and the diameter study summarized above indicate that the nature of the body interaction effects on the phase and amplitude of the system response are impacted more by the diameter of the human body than its height, indicating that real-world implementations of the system may require calibration that considers the stature of the user.

3) Body Composition: The nominal body dielectric constant is 60 [11]. To study the effects of this parameter on the amplitude and phase response of the system, dielectric constants of 20, 40, and 80 are compared to the nominal configuration. The frequency-dependent phase and amplitude response perturbations due to the varied body height are provided in Figure 10(a) and Figure 10(b), respectively.

Somewhat surprisingly, these results indicate that the performance of the direction finding system is likely to be relatively insensitive to the composition of the human body, even though the range of constitutive parameters is very large. As previously discussed, the dielectric properties of the human body are dependent on both body composition and frequency. This result is significant, because it indicates that it is the presence of the body that is more important to changing the system dynamics than its specific composition or the signals it is being used to detect.

C. System Parameters

1) Antenna Baseline Separation: The nominal antenna baseline is 20". To study the effects of this parameter on the amplitude and phase response of the system, antenna baselines of 18" and 22" are compared to the nominal configuration. The frequency-dependent phase and amplitude response perturbations due to the varied antenna baseline separation are provided in Figure 11(a) and Figure 11(b), respectively.

The separation between sensors in a direction finding system has a significant impact on the performance of the system. This phenomenon is confirmed by this study, which indicates that the relative separation of the sensors (not only from one another, but also from the

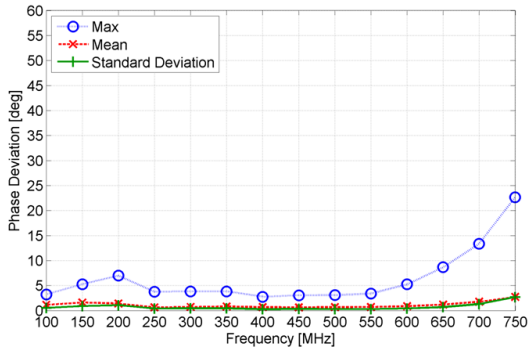

(a) Phase response perturbation.

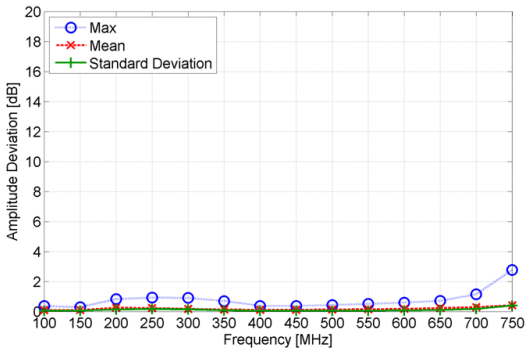

(b) Amplitude response perturbation.

Figure 10. System response to variations of the body composition.

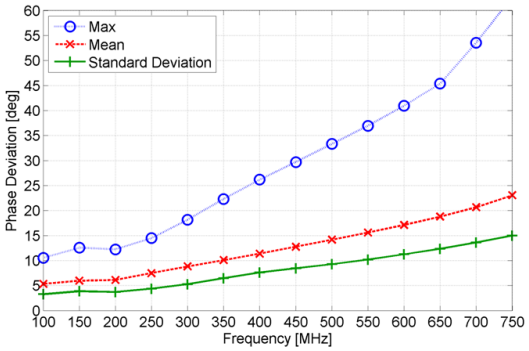

(a) Phase response perturbation.

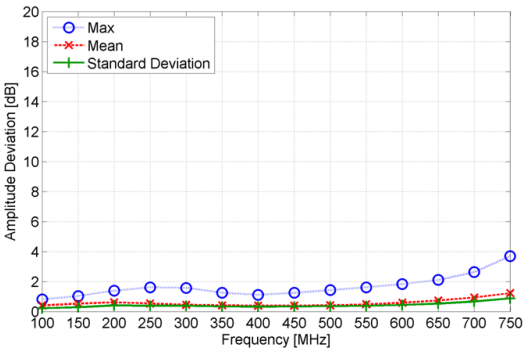

(b) Amplitude response perturbation.

Figure 11. System response to variations of the antenna baseline separation.

human body) does indeed produce a significant change in the system response. The electrical spacing of the antennas changes the relative time of arrival at signals at the two sensors, accounting for the frequency-dependent effect in the phase response. Somewhat surprisingly, the amplitude response is relatively insensitive to the antenna spacing. In many real-world realizations of this system, this baseline may be mechanically fixed to avoid the perturbations observed here.

2) Antenna Baseline Rotation: The nominal antenna baseline oriented parallel to the y-axis. To study the effects of this parameter on the amplitude and phase response of the system, antenna baseline rotations of 5° and 10° are compared to the nominal configuration. The rotational symmetry of the problem precludes the need to study negative rotation values. The frequency-dependent phase and amplitude response perturbations due to the varied antenna baseline rotation are provided in Figure 12(a) and Figure 12(b), respectively.

In the baseline configuration, the antennas are located on the y-axis, perpendicular to the orientation of the user. In real-world applications, it may be possible for the antennas to rotate somewhat with respect to the user. As confirmed by this study, there is a significant perturbation in the system performance if the sensors rotate. The direction finding solution generated by the system is referenced to the sensor geometry, so the anticipated result of this rotation is an error in the direction finding solution that is comparable to the rotation of the antennas with respect to the body. However, unlike free space realizations of comparable direction finding systems, this rotation also changes the proximity of the sensors to the body, so additional effects are also expected. The maximum perturbations observed in this study are approximately 121° for the phase and 8.2dB for the amplitude. However, at over 5σ each, these perturbations are relatively uncommon, as reflected in the low mean and standard deviation values.

3) Antenna Height on Body: The nominal antenna position is in the middle of the cylindrical body along the z-axis. To study the effects of the positional offset on the amplitude and phase response of the system, antenna baseline heights of 12" and 24" above the nominal plane are computed. The vertical symmetry of the problem precludes the consideration of negative antenna heights. The frequency-dependent phase and amplitude response perturbations due to the varied antenna baseline height are provided in Figure 13(a) and Figure 13(b), respectively.

In the baseline configuration, the sensors are centered at the "equator" of the cylindrical body model.

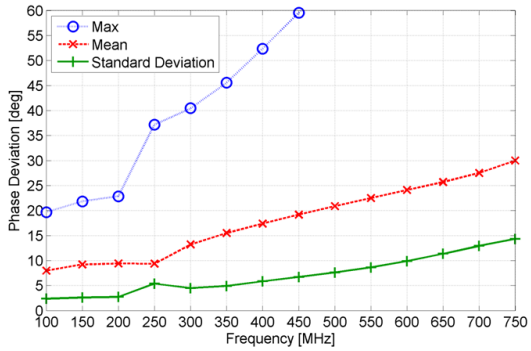

(a) Phase response perturbation.

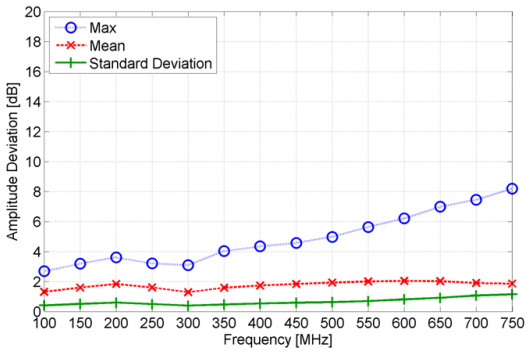

(b) Amplitude response perturbation.

Figure 12. System response to variations of the antenna baseline rotation.

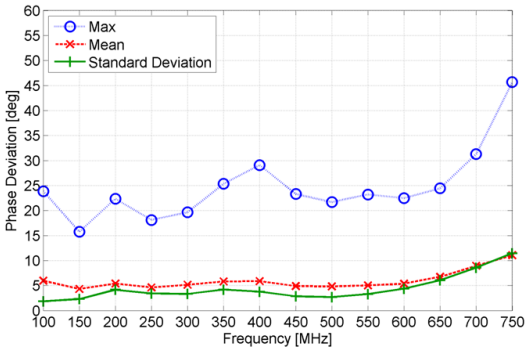

(a) Phase response perturbation.

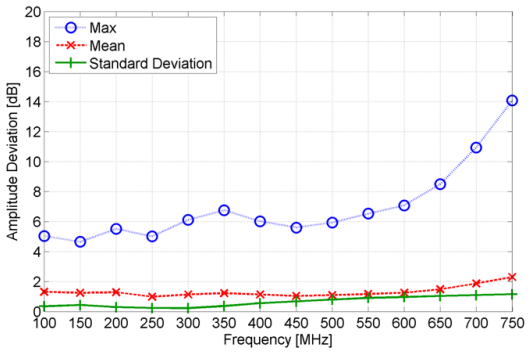

(b) Amplitude response perturbation.

Figure 13. System response to variations of the antenna baseline height.

Although this configuration may not be realistic for real-world applications, the study summarized here indicates that even large vertical perturbations in the location of the sensors with respect to the body model produce relatively minor perturbations to the phase and amplitude of the system response. In fact, the largest perturbation in phase (approximately 45.5° is over 3σ away from the mean, and the largest perturbation in the amplitude (14dB) is over 10σ above the mean. Much like the results of the body height study, these results indicate that there is relatively little system sensitivity on the relative vertical orientation of the body and the sensors.

4) Left/Right Body Centrality: The nominal body location is centered in the y-axis. To study the effects of this parameter on the amplitude and phase response of the system, left/right (y-axis) body offsets of 1" and 2" are compared to the nominal configuration. The symmetry of the problem makes the use of negative offset values unnecessary. The frequency-dependent phase and amplitude response perturbations due to the varied y-axis body offset are provided in Figure 14(a) and Figure 14(b), respectively.

The performance of the baseline direction finding system is significantly changed in the presence of the body. Given the close electrical proximity of the body ($d \ll \lambda$) to the sensors, the sensitivity of the system response that is associated with changing the location of the body relative to the sensors is important to the stability of the system. The results from this study confirm that slight changes in the relative positions of the sensors and the body may produce significant changes in the nominal system performance.

5) Forward/Backward Body Centrality: The nominal body location is offset from the origin by $+10$" in the x-axis. To study the effects of this parameter on the amplitude and phase response of the system, forward/backward (x-axis) body offsets of 8" and 12" are compared to the nominal configuration. The frequency-dependent phase and amplitude response perturbations due to the varied x-axis body offset are provided in Figure 15(a) and Figure 15(b), respectively.

As with the left/right centrality study, this study confirms that the performance of the baseline direction finding system is significantly influenced by the proximity of the sensors to the body. Between these studies, the most pronounced variation is exhibited by the phase response on the forward/backward sensitivity, where $\sigma_{max} \approx 15^\circ$.

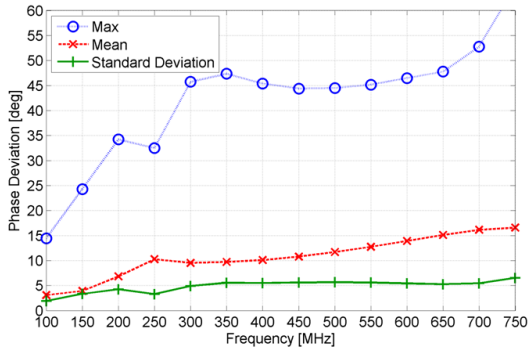

(a) Phase response perturbation.

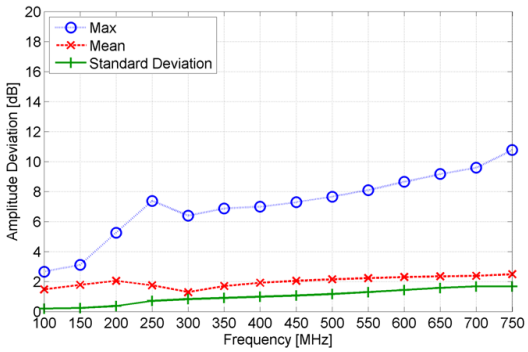

(b) Amplitude response perturbation.

Figure 14. System response to variations of the y-axis body offset.

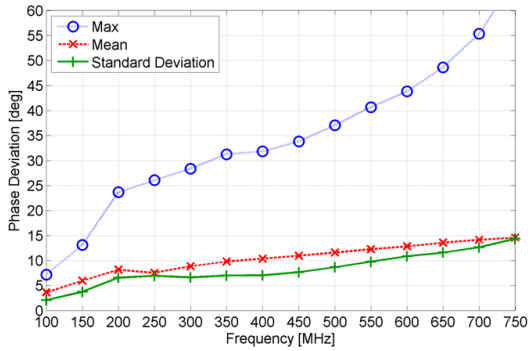

(a) Phase response perturbation.

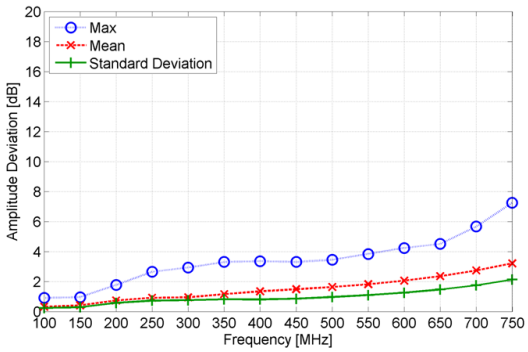

(b) Amplitude response perturbation.

Figure 15. System response to variations of the x-axis body offset.

D. Excitation Parameters

1) Off-Horizon Signals: The nominal signals of interest reside in the terrestrial plane ($\theta = 90°$). To study the effects of this parameter on the amplitude and phase response of the system, θ values of $105°$ and $120°$ are compared to the nominal configuration. The vertical symmetry of the problem renders above-horizon elevation angle values unimportant to this study. The frequency-dependent phase and amplitude response perturbations due to the varied signal elevation angle are provided in Figure 16(a) and Figure 16(b), respectively.

The phase and amplitude of the currents excited on the sensor depend on the signal's electric field, all scattered modes/fields, and electric field modes supported by the antenna [13]. Accordingly, there is an anticipated change in the system performance when signals arrive from elevation angles away from the azimuthal plane. Although most signals detected by real-world implementations of this system are most likely to arrive from angles within a few degrees of this plane, this study identifies that the system will produce a somewhat different response to signals that are significantly away from the azimuthal plane.

2) Signal Polarization: The nominal signals of interest are vertically polarized. To study the effects of this parameter on the amplitude and phase response of the system, slant-$45°$ and horizontally polarized signals are compared to the nominal configuration. The frequency-dependent phase and amplitude response perturbations due to the varied signal polarization are provided in Figure 17(a) and Figure 17(b), respectively.

The vertically oriented dipoles used as the system's sensors are vertically polarized. As expected, the perturbation in the system response due to signal polarization is considerable. Specifically, as the signal polarization rotates away from vertical, the system's ability to detect the signal diminishes accordingly. When the signals are slant-polarized, both sensors have an equivalently-diminished ability to detect the signals, and there is little variation in the system, resulting in the very standard deviation values. However, when the signals are horizontally polarized, neither sensor is able to detect the signal well, and there is an unpredictable response, resulting in the large mean and maximum perturbation metrics. Most terrestrial signals are vertically polarized, however, this study identifies the limited nature of the system performance for detecting those signals that are not co-polarized with the sensors.

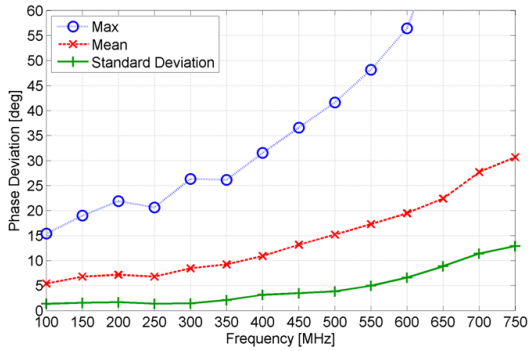

(a) Phase response perturbation.

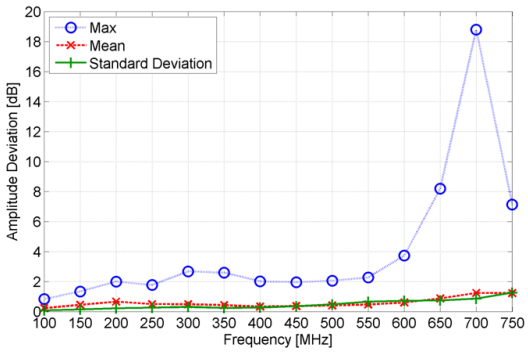

(b) Amplitude response perturbation.

Figure 16. System response to variations of the signal elevation angle.

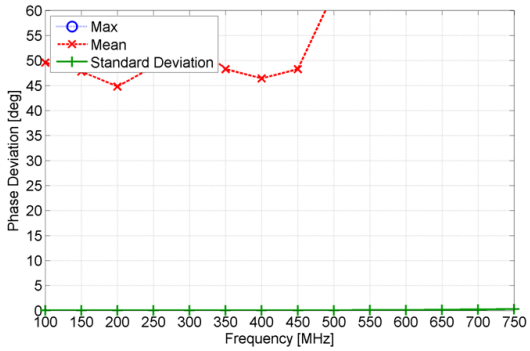

(a) Phase response perturbation.

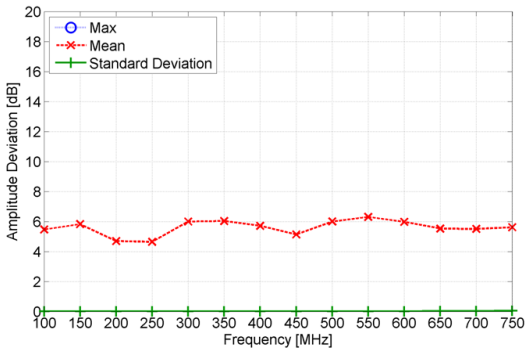

(b) Amplitude response perturbation.

Figure 17. System response to variations of the signal polarization.

E. Detection Thresholds

To combine the results of these studies, frequency-dependent data are collected for the relative phase and amplitude of the response of the direction finding system when seven of the twelve variables are independently perturbed. The seven variables that are selected are body diameter, body height, left/right and forward/backward body centrality, baseline rotation, height on body, and body dielectric constant. These variables represent parameters that are likely to vary among users and with normal user movement. The five variables that are excluded are signal polarization, signal elevation angle, radiator termination impedance, radiator height, and baseline separation. These variables are excluded from this evaluation because they represent fundamental changes to the system that are not likely in the field, or would require a complete recalibration of the system.

As previously discussed, the system response at each frequency is a function of incidence angle. To represent the distribution of the perturbation of the system response across all angles of incidence effectively, these data are consolidated. Specifically, if the angular perturbations are considered to lie in some distribution, it is most convenient to describe the shape of this distribution. Accordingly, the standard deviation of the angular perturbations is collected as a function of frequency. These data are plotted in Figure 18.

Data from these studies are useful to establish thresholds in phase and amplitude perturbation that will be used to detect incoming signals. Signal perturbations below the levels observed in this study will be ignored by the system, and attributed to slight changes in the system geometry (e.g. due to different users or user movement). Signal perturbations above these levels will be attributed to differences in incoming signals, and will be used to identify these signals and generate direction finding solutions. In these plots, it is clear that there is a frequency dependence in the perturbation of the phase and amplitude of the system response: higher levels of perturbation are seen at higher frequencies. Broken gray lines at approximately 14.5° in Figure 18(a) and just below 2.5dB in Figure 18(b) are used to indicate the maximum signal deviations among each of the selected studies. To simplify the broadband implementation of direction finding techniques, nominal frequency-independent detection thresholds of 10° and 2dB are selected for all frequencies. As highlighted by the "dot-dash" gray lines in Figures 18(a) and 18(b), these threshold levels capture most of the observed deviation values across most of the band of interest. Different techniques for selecting these thresholds are

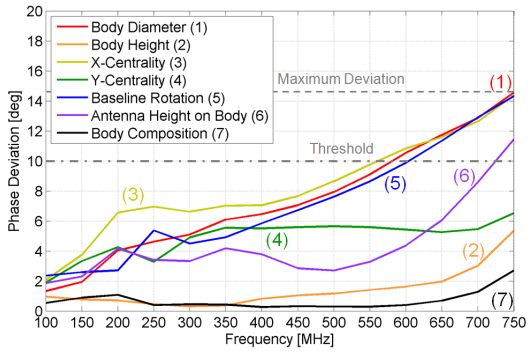

(a) Relative phase perturbation.

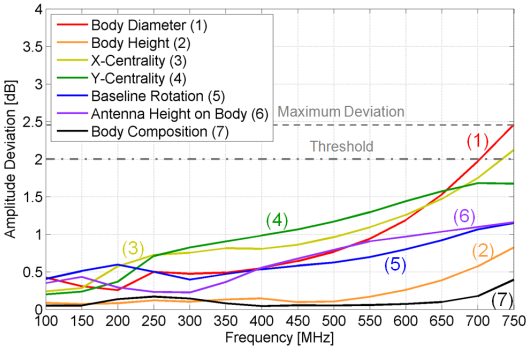

(b) Relative amplitude perturbation.

Figure 18. Relative phase and amplitude perturbations from the sensitivity study.

discussed in Section 5.

IV. Direction Finding Calibration

Having established means of discriminating different signals from one another, it is possible to perform analysis on the performance of the direction finding system. To do so, an auto-correlating direction finding function [7] is used to calibrate the system responses. In this technique, the system response of the direction finding system is auto-correlated using a procedure that produces a correlation error called a direction finding function (DFF). The auto-correlation function uses the spatial signal response, $S(\phi)$, as its input, and identifies parts of the signal that match one another. If the signal is one-to-one, each part of the signal only correlates with itself. If it is not one-to one, multiple portions of the signal will correlate, identifying ambiguities.

For a signal incident from known angle ϕ_0, the auto-correlation is defined in 1.

$$DFF_{\phi_0}(\phi) \equiv S(\phi_0) - S(\phi) \tag{1}$$

The output of the auto-correlation function is identically equal to 0 when $\phi = \phi_0$, indicating a proper identification of a signal. However, it is possible that other angles may also minimize the DFF, producing false alarms. The output of this direction finding function at 100 MHz is shown for three different incidence angles in Figure 19(a) and Figure 19(b), using phase and amplitude system responses, respectively, as the input.

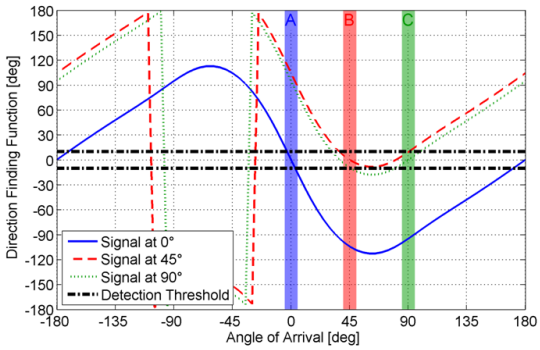

(a) The phase direction finding function.

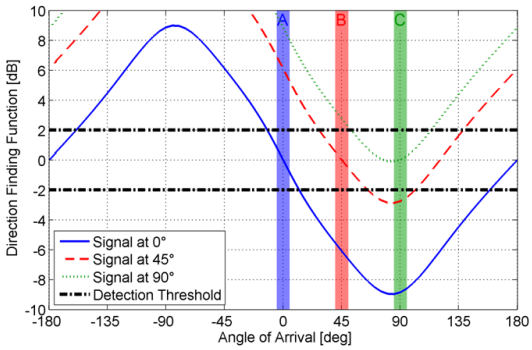

(b) The amplitude direction finding function.

Figure 19. Characterization the phase and amplitude of the system response by the direction finding function.

Note that the three shaded bands on the plots in Figure 19 highlight the areas where the three signals should have zero error (DFF = 0). Indeed, the center of the blue shaded band (labeled "A") highlights the proper angle for the blue line (0°), the center of the red shaded band (labeled "B") highlights the zero-crossing of the red line (45°), and the center of the green shaded band (labeled "C") highlights the zero-crossing of the green line (90°). However, ambiguities are also seen for the incident signals at 0° and 45°. The blue line (0°) has a zero crossing at $\phi_0 = 0°$, but another at $\phi_0' = \pm 180°$. The red line (45°) has a zero crossing at ($\phi_0 = 45°$, and a false return at $\phi_0' \approx 120°$ in the phase response, but no false return in the amplitude response.

These data indicate that the phase and amplitude responses can be used to independently generate a direction finding solution. Both approaches are able to identify the proper location of the signal, but may be susceptible to

different ambiguities. An approach to combine these solutions is presented in [14], [15], and is shown to provide better performance than either individual approach.

V. Conclusion

In this work, a baseline computational model of a body-borne direction finding system is established. MoM simulations of this system are shown to have excellent agreement with measured data. A parametric system response study is conducted to identify the stability of the system to real-world perturbations. The level of these perturbations is used to establish frequency-independent thresholds that are used by the phase-based and amplitude-based direction finding systems to determine the angle of arrival of incident signals. Based on these data, a calibration technique is used to characterize the performance of the direction finding system, and identify associated ambiguities.

When considered together with the results of the body height and diameter studies, the results of the body composition study indicate that real-world implementations of the system may require specific calibration for different sized users, but will not be susceptible to variations in the user's body composition or the frequency of incoming signals. The raw system response (relative phase and amplitude) is consolidated for signals across all angles of arrival to identify those variables that have the most significant impact on the system. Real-world implementations of the system should be able to control many of these parameters, such as radiator height and separation. However, others may change considerably depending on the user, such as body height and diameter, baseline rotation, and the relative location of the body and the sensors.

A more rigorous theoretical and/or statistical analysis of the perturbation data is recommended for the determination of real-world detection thresholds. Because the focus of this paper is on the computational characterization of the body-borne system, nominal frequency-independent detection thresholds are selected using the data from the parametric system response. These conservative thresholds are useful to highlight their application to a direction finding calibration technique, but do not represent optimized values. Additional work by the authors [14], [15] provides a more thorough description of how the direction finding function can be applied to optimize the performance of a direction finding system. Using the direction finding approach described in the referenced paper, the phase and amplitude detection thresholds can be optimized for various metrics, including accuracy, sensitivity, and false alarm rates.

The results of this study clearly demonstrate the utility of a method of moments in the characterization of direction finding systems. This includes the accurate replication of body-interaction effects that are observed in measurements. Future examinations based on this work include coupled/multivariable sensitivity studies, improvement of the direction finding calibration, and the extension of the direction finding technique to geolocation applications.

References

[1] S. E. Lipsky, *Microwave Passive Direction Finding*. SciTech, Incorporated, 2003.

[2] H. de A. Donisthorpe, "The Marconi Marine Radio Direction Finder," *Proceedings of the Institude of Radio Engineers*, vol. 13, no. 1, pp. 29–47, 1925.

[3] P. Misra and P. Enge, *Global Positioning System - Signals, Measurements, and Performance*. Ganga-Jamuna Press, 2 ed., 2006.

[4] P. Enge, E. Swanson, R. Mullin, K. Ganther, A. Bommarito, and R. Kelly, "Terrestrial Radio Navigation Technologies," *Navigation*, vol. 42, no. 1, pp. 61–108, 1995.

[5] H. Jenkins, *Small-Aperture Radio Direction-Finding*. Artech House Publishers, 1991.

[6] EM Software & Systems, "FEKO." Commercially Licensed Software, 2008.

[7] A. Bellion, C. L. Meins, A. Julien-Vergonjanne, and T. Monédière, "Generation of Calibration Tables for Direction Finding Antennas Using FEKO," *24th Annual Review of Progress in Applied Computational Electromagnetics (ACES)*, pp. 903–908, 2008.

[8] N. Uzunoglu, P. Cottis, and P. Papakonstantinou, "Analysis of Thermal Radiation from an Inhomogeneous Cylindrical Human Body Model," *IEEE Trans. Microwave Theory and Techniques*, vol. MTT-35, pp. 761–768, 1987.

[9] P. Cottis, G. Chatzarakis, and N. Uzunoglu, "Electromagnetic Energy Deposition Inside a Three-Layer Cylindrical Human Body Model Caused by Near-Field Radiators," *IEEE Trans. Microwave Theory and Techniques*, vol. MTT-38, pp. 990–999, 1990.

[10] K. Gryz, J. Karpowicz, and S. Wincenciak, "Numerical Modeling of Current Flowing in Human Exposed to External Electric Field for Evaluation of Occupational Exposure," *Proceedings of the URSI General Assembly*, 2002.

[11] Y.-M. Gimm and Y.-J. Ju, "Formulation of the Sugar-Free Human Head Tissue Simulant Liquid for SAR Measurement at 830 MHz," in *Proceedings of the Asia-Pacific Radio Science Conference*, pp. 533–536, 2004.

[12] J. L. Devore, *Probability and Statistics for Engineering and the Sciences*. Duxbury Press, 6 ed., June 2003.

[13] W. L. Stutzman and G. A. Thiele, *Antenna Theory and Design*. John Wiley & Sons, second ed., 1998.

[14] A. Lalezari, F. Lalezari, B. Jeong, and D. Filipović, "Evaluation of Human Body Interaction for the Enhancement of a Broadband Body-Borne Radio Geolocation System," *Proceedings of the Allerton Antenna and Application Symposium*, pp. 436–453, 2008.

[15] A. C. Lalezari, "Exploitation of Body Interaction Effects for the Enhancement of a Body-Borne Radio Geolocation System," Master's thesis, University of Colorado at Boulder, December 2008.

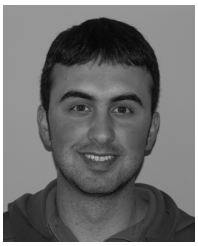

Arian Lalezari received the B.S. degrees in Electrical Engineering and Applied Mathematics from the University of Colorado in 2005, and the M.S.E.E. degree from the University of Colorado at Boulder in 2008.

Since 2004, he has been working at FIRST RF Corporation in Boulder, CO. At FIRST RF, Mr. Lalezari is currently working on man-portable, low-profile/conformal, satellite communications, and radar antennas.

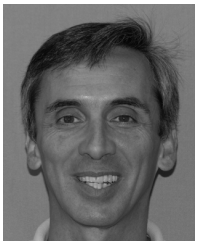

Farzin Lalezari received the B.S.E.E. and the M.S.E.E degrees from the Polytechnic Institute of Brooklyn in 1976 and 1977, respectively, and completed course work for the PhD degree from the University of Colorado at Boulder from 1977-1978.

Mr. Lalezari is the Principal Engineer for FIRST RF Corporation. He has more than 28 years of experience in antennas and RF systems design. He has a current Top Secret SSBI security clearance. Additionally, Mr. Lalezari has over 25 patents issued or pending in this field of research. He is responsible for engineering development tasks on government R&D contracts relating to aerospace and defense applications and development of advanced Radio Frequency (RF) technologies including: antennas, antenna systems, electronic warfare (EW) and threat neutralization, algorithms, overall system development for communications, navigation, identification, guidance and control, pointing and control, weapons seekers and fuzing, telemetry, and remote sensing.

Dejan Filipović received the Dipl. Eng. degree in electrical engineering from the University of Nis, Serbia in 1994, and the M.S.E.E. and PhD degrees from the University of Michigan, Ann Arbor in 1999 and 2002 respectively. From 1994 to 1997, he was a Research Assistant at University of Nis. From 1997 to 2002, he was Graduate Student at the University of Michigan. Currently, he is Associate Professor at the University of Colorado, Boulder. His research interests are in the development of mm-wave components and systems, multi-physics modeling, antenna theory and design, as well as in computational and applied electromagnetics.

Mr. Filipović was the recipient of the prestigious Nikola Tesla Award for his outstanding graduation thesis. He and his students were co-recipients of the Best Paper Award presented at the IEEE Antennas and Propagation Society (AP-S)/URSI and Antenna Application Symposium conferences.